PFI-ZEKE photoelectron spectroscopy of positively charged ions: illustration with Mg+

Author(s):
Génévriez, Matthieu; Wehrli, Dominik; Agner, Josef A.; Merkt, Frédéric

Publication date:
2019-01

Permanent link:
https://doi.org/10.3929/ethz-b-000307574

Originally published in:
International Journal of Mass Spectrometry 435, https://doi.org/10.1016/j.ijms.2018.10.017

Funding acknowledgement:
172620 - Precision measurements with cold molecules: Rydberg states, ions and photoionization (SNF)
743121 - Cold Ion Chemistry - Experiments within a Rydberg Orbit (EC)

The following article appeared in *J. Mass. Spectrom.* **435**, 209 (2019) and may be found at https://doi.org/10.1016/j.ijms.2018.10.017.

PFI-ZEKE photoelectron spectroscopy of positively charged ions: illustration with Mg^+

M. Génévriez[a], D. Wehrli[a], J. A. Agner[a], F. Merkt[a]

[a] *Laboratory of Physical Chemistry, ETH Zurich, CH-8093 Zurich, Switzerland*

Abstract

Pulsed-field-ionization zero-kinetic-energy (PFI-ZEKE) photoelectron spectroscopy has been applied for the first time to a positively charged ion, Mg^+. Mg^+ ions have been prepared in the [Ne]3s $^2S_{1/2}$ ground state by photoionization of Mg atoms in a supersonic expansion. The ions were then excited to very high Rydberg states located just below the ionization threshold corresponding to the formation of ground-state Mg^{2+} by (2+1′) resonance-enhanced three-photon absorption via the 3d $^2D_{5/2}$ intermediate state. We demonstrate experimentally and in a calculation of the transition moments that only the nf Rydberg series of Mg^+ is efficiently excited from the $^2D_{5/2}$ state and extract from the Rydberg spectrum precise values for the ionization energy of Mg^+ (121267.65 ± 0.06 cm^{-1}) and the quantum defect of the nf series (0.0044(6)). The field ionization of very high Rydberg states of Mg^+ was investigated using sequences of electric pulses. Compared to the pulsed field ionization of neutral atoms or molecules, the pulsed field ionization of positively charged ions differs in three respects: (i) The shift of the ionization thresholds induced by an electric field of given strength is larger by a factor of approximately $\sqrt{2}$, (ii) the inherent presence of ions in the photoexcitation volume prevents the escape of slow electrons, and (iii) the inhomogeneous stray fields induced by these ions and their effects on the high Rydberg states reduce the selectivity of the field-ionization process and degrade the resolution of the PFI-ZEKE photoelectron spectra. By minimizing the ion density, optimizing the photoexcitation efficiency and using multipulse field-ionization sequences, we show that the resolution of the photoelectron spectra can be as high as 0.3 cm^{-1}, which opens up the possibility to study doubly-charged cations by high-resolution photoelectron spectroscopy.

1. Introduction

Doubly-charged cations, also called dications in the following, are interesting objects for investigations by high-resolution spectroscopy. The structural and dynamical properties of dications subtly depend on the balance between

chemical-bonding interactions and the repulsive Coulomb interaction that determines the long-range part of the potential-energy surfaces at the separated-ions limit. This competition gives rise to a broad range of behaviors that can be classified in five prototypical limiting cases, designated (a)-(e) in the classification scheme of Schröder and Schwarz [1] (see their figure 2). The scheme includes two different limiting cases of thermodynamic stability [(a) and (b)] and of metastability [(c) and (e)] depending on the relative positions of the potential curves correlated asymptotically to two singly-charged fragments or to a neutral and a doubly-charged fragment. Numerous doubly charged cations of diatomic molecules and small polyatomic molecules are known to be stable or metastable [1, 2, 3], the evidence being provided primarily by ab-initio quantum-chemical calculations, or experimental investigations by mass spectrometry and coincidence photoelectron spectroscopy above the double ionization threshold of neutral molecules (see Ref. [4] and references therein).

The experimental methods used to generate dications include electron-impact ionization, double-photoionization, electrospray ionization, charge stripping, and double charge transfer [1, 3]. The first two methods simultaneously provide information on the ionization thresholds, and in the case of double photoionization even on the vibronic level structure of dications (see, e.g., Refs. [5, 6] for selected examples of vibrationally resolved coincidence photoelectron spectra). Structural information on dications can also be derived by measuring and analyzing the kinetic-energy distribution of the charged fragments released upon dissociation (see, e.g., Ref. [7]).

High-resolution spectroscopic data on molecular dications are extremely scarce in the literature (see Refs. [8, 9] for notable examples). PFI-ZEKE photoelectron spectroscopy seems ideally suited to fill this gap, but has not been applied yet to singly charged cations. The main reason is not the restriction, by space-charge effects, of the density of charged species in the gas phase. Threshold photoelectron spectroscopy and related techniques have indeed been successfully used in high-resolution spectroscopic studies of singly-charged anions (see [10] for a recent review). It is more likely to be the high photon energies required to reach the ionization thresholds. Rapid progress is currently being made in the development of intense short-wavelength radiation sources and one can anticipate that this progress will soon result in spectroscopic studies of molecular dications at a resolution sufficient to observe their rotational structure. In this article, we demonstrate the use of PFI-ZEKE photoelectron spectroscopy [11] to study the photoelectron spectra of singly-charged atomic cations at high spectral resolution and characterize experimentally the differences that arise compared to studies of neutral molecules and atoms with this technique.

PFI-ZEKE photoelectron spectroscopy relies on the pulsed, monochromatic photoexcitation of an atomic or molecular system to long-lived Rydberg states of very high principal quantum number n ($n \geq 200$) located just below each ionization threshold, followed by their ionization with a delayed pulsed electric field [11, 12, 13, 14]. The delay between photoexcitation and pulsed field ionization acts as an efficient energy filter because the electrons emitted by direct

ionization or autoionization either fly out of the photoexcitation volume or are swept out of it by stray electric fields. A spectrum is recorded by monitoring the field-ionization yield as a function of the excitation frequency. In laser-based experiments, the resolution is usually not limited by the bandwidth of radiation used for photoexcitation, but by the electric field pulses used for field ionization.

The low frequency onset of a field-ionization signal with respect to the field-free ionization threshold, which corresponds to the field-induced shift ΔE_{I} of this threshold, is proportional to the square root of the electric field strength F [15, 16]

$$\Delta E_{\mathrm{I}}/(hc\,\mathrm{cm}^{-1}) = -c\sqrt{F/(\mathrm{V/cm})}, \tag{1}$$

where c is a unitless proportionality coefficient and the units of cm^{-1} and V/cm are used for the excitation wave number and the electric field strength, respectively. In the simplest, classical model to describe field-induced shifts, the potential $V(\mathbf{r})$ at the position $\mathbf{r}$ of the Rydberg electron has contributions arising from the ion core with charge Z_{c} and from the applied electric field. Choosing the z axis of the coordinate system to coincide with the direction of the electric field vector and its origin to be at the position of the ion core results in

$$V(\mathbf{r}) = -\frac{Z_{\mathrm{c}}e^2}{4\pi\epsilon_0 r} - eFz. \tag{2}$$

The saddle point (sp) in this potential is located at

$$z_{\mathrm{sp}} = \sqrt{\frac{e}{4\pi\epsilon_0 Z_{\mathrm{c}}F}};\; V_{\mathrm{sp}} = -\frac{2e^{3/2}\sqrt{Z_{\mathrm{c}}F}}{\sqrt{4\pi\epsilon_0}}, \tag{3}$$

which corresponds to a value of $c = 6.12\sqrt{Z_{\mathrm{c}}}$ in Eq. (1) and adequately describes the thresholds observed in the photoionization of neutral systems ($Z_{\mathrm{c}} = 1$) [13, 14] in the presence of static electric fields. When pulsed electric fields are used, one needs to consider the ionization dynamics in the time-dependent electric field. For the high-n Rydberg states detected in PFI-ZEKE photoelectron spectra and pulsed-field rise times of a few tens of nanoseconds, the field ionization follows a diabatic mechanism [15, 16, 13, 14]. In typical single-pulse experiments the mid-rise position of the low-frequency edge of the field-ionization signal, and thus the spectral resolution, is usually well described, in neutral systems, by Eq. (1) with $c \approx 4$ [13]. Multipulse sequences lead to a higher resolution than single pulses (about 0.1 cm^{-1} [17]) and the widths and positions of the observed lines can be modeled accurately by assuming a diabatic field-ionization mechanism (see Ref. [17] for details). Based on the classical field-ionization model described above, one would expect that the signal onsets and field-induced shifts scale with $\sqrt{Z_{\mathrm{c}}F}$ and that the observations made in studies by PFI-ZEKE photoelectron spectroscopy of neutral systems can be adapted to singly-charged ions multiplying all shifts by $\sqrt{2}$. For a given pulse sequence, the resolution of PFI-ZEKE photoelectron spectra of singly-charged ions should thus degrade by a factor of $\sqrt{2}$. To anticipate the results presented in Section 3.1, our observations confirm these predictions qualitatively. However,

the fact that the experiments are carried out with ions impose restrictions on the field-ionization pulse sequences and limit the resolution to about 0.3 cm^{-1}.

2. Experimental setup and procedure

The experimental setup, sketched in Fig. 1(a), consists of a pulsed laser-ablation supersonic-expansion source, three Nd:YAG-pumped pulsed dye lasers and a PFI-ZEKE photoelectron/photoion spectrometer. The experiments are carried out in a pulsed mode at a repetition rate of 25 Hz.

The design of the ablation source is similar to that described by Powers *et al.* [18]. In the source chamber, light pulses from a frequency-doubled, Q-switched Nd:YAG laser are used to ablate the surface of a Mg rod. Ablation occurs within the nozzle of a pulsed supersonic expansion source and the ablated species, predominantly magnesium atoms, are entrained in the N_2 carrier gas released by the pulsed valve. The supersonic beam is then collimated by a 4-mm-diameter skimmer located 8 cm downstream from the valve orifice, before it enters the photoexcitation chamber. The magnesium rod is constantly rotated and translated by a screw-drive mechanism so as to ablate a fresh area at every laser shot. The ablation-laser beam is attenuated by the combination of a $\lambda/2$ plate and a polarizer and focused by an $f = 30$ cm lens located outside of the source chamber. It reaches the rod after passing through a 1.5 mm hole drilled in the side of the nozzle. An optimal compromise between a long rod lifetime and a sufficient ablated-atom density was reached by keeping the laser pulse energy below ~ 6 mJ and setting the position of the lens focus slightly beyond the rod. The relative fluctuation of the intensity of the measured signals, averaged over 50 laser shots, is of the order of 10%, with variations resulting primarily from the fluctuation of the density of magnesium atoms in the beam generated by the ablation process itself. Long-term drifts and single-pulse bursts of the Mg density are also observed and attributed to spatial variations in the quality of the rod surface and local defects, respectively.

In the photoexcitation chamber, the magnesium beam is intersected at right angles by the light pulses from three dye lasers, the first of which ionizes the Mg atoms while the latter two either excite the ground state Mg^+ ions ($[Ne](3s)^1\ ^2S_{1/2}$) to Rydberg states or photoionize them. The corresponding multiphoton, resonance-enhanced ionization and excitation scheme is schematically depicted in Fig. 1(b). The three lasers are pumped by the same frequency-doubled, pulsed and seeded Nd:YAG laser, and their outputs are either frequency-doubled or tripled using β-barium borate (BBO) crystals. Their respective wavenumbers are measured using a commercial wavemeter with a specified absolute accuracy of 0.02 cm^{-1}.

The first laser, called laser 1 hereafter, is a commercial pulsed dye laser with a bandwidth of 0.12 cm^{-1} and operated with the dye Rhodamine 6G. Its wavenumber is set so that, after frequency-doubling, the UV radiation drives the $3s^2\ ^1S - 3s3p\ ^1P$ transition of neutral magnesium ($\tilde{\nu}_1 = 35051.26$ cm^{-1} [19]), as shown in Fig. 1(b). The atoms are then ionized by absorption of a second photon. This 1+1 REMPI scheme provides large photoionization efficiencies, and

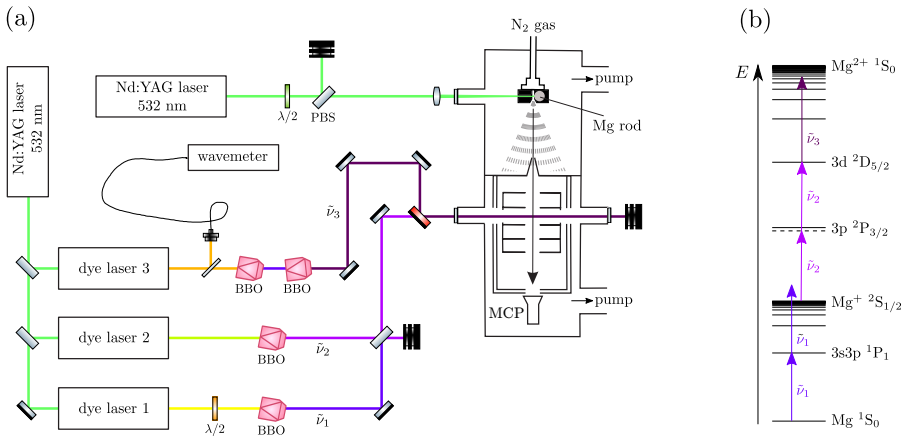

Figure 1: (a) Experimental setup. BBO: β-barium borate crystals; $\lambda/2$: half-wave plate; PBS: polarizing beam splitter; MCP: micro-channel plates detector. (b) Schematic view of the relevant energy levels of the magnesium atom, singly- and doubly-charged ions, and photoexcitation scheme.

thus efficient production of Mg^+ ions in their ground state ($3s\ ^2S_{1/2}$). Moreover, it allows one to adjust the concentration of Mg^+ ions in the beam by changing the laser pulse energy. This is achieved by rotating the polarization of the fundamental output of the dye laser with a $\lambda/2$ plate before the frequency-doubling crystal, thus changing the frequency-doubling efficiency.

The second and third lasers, called lasers 2 and 3 below, are commercial, double-grating, pulsed dye lasers operated with the dye Rhodamine 6G and with a mixture of the dyes Rhodamine 101 and Rhodamine B, respectively. Their bandwidth is about 0.05 cm^{-1}. The frequency-doubled output of laser 2 is tuned to $\tilde{\nu}_2 = 35745.10\ cm^{-1}$, matching the wavenumber of the two-photon $Mg^+(3s\ ^2S_{1/2}) - Mg^+(3d\ ^2D_{5/2})$ transition [19]. Fortuitously, this wavenumber is only about 16 cm^{-1} below that of the one-photon $Mg^+(3s\ ^2S_{1/2}) - Mg^+(3p\ ^2P_{3/2})$ resonance, and therefore the two-photon transition probability to the $3d\ ^2D_{5/2}$ state is strongly enhanced. The output of laser 3 is frequency-tripled using two BBO crystals for successive frequency-doubling ($2\tilde{\nu}_{f3}$) and sum-frequency mixing ($\tilde{\nu}_3 = 2\tilde{\nu}_{f3} + \tilde{\nu}_{f3}$). Both BBO crystals are mounted on high accuracy, servo-controlled rotation stages and rotated according to the wavenumber of the fundamental beam, thus providing tunable radiation in the range $49500 - 50000\ cm^{-1}$ needed for the excitation to high-n Rydberg states.

The three laser beams are overlapped spatially using the combination of a 50/50 beamsplitter and a dichroic mirror and traverse the photoexcitation chamber *via* quartz laser windows. The 4-ns-long pulses from lasers 2 and 3 are delayed by 8 ns with respect to the 4-ns-long pulses from laser 1 using an optical delay line. The diameters of each beam in the interaction region are $\sim$1 mm and were determined by moving a razor blade, mounted on a translation stage, across the beam and measuring the transmitted energy as a function of the

blade position.

The interaction region is surrounded by a 5.8-cm-long stack of five cylindrical, equally-spaced and resistively-coupled electrodes. Pulsed electric potentials of either polarity can be applied to the stack to generate the electric fields required for the field ionization of the Mg^+ Rydberg states and the extraction of electrons or Mg^{2+} ions. The charged particles are then detected at the end of a linear time-of-flight (TOF) tube using a microchannel-plate (MCP) detector. The MCP signal is amplified and measured on a fast oscilloscope, itself connected to a computer for data recording and analysis. The electrode stack and TOF regions are surrounded by two concentric mu-metal shields to suppress stray magnetic fields.

When detecting ions, such as for the Rydberg spectrum presented below in Fig. 2, a square pulse of +3 kV is applied to the electrode stack, with a delay of $\sim$ 50 ns with respect to the laser pulses. This pulsed electric field ionizes Mg^+ ions which are in Rydberg states with principal quantum number larger than 50 and extracts all positively-charged particles. Mg^{2+} ions are then separated from Mg^+ ions in the TOF tube. In the TOF spectra, the three stable magnesium isotopes, with masses 24, 25 and 26 u, are well separated and the measured abundances match the natural ones (79%, 10% and 11% respectively). A small isotopic shift ($\lesssim 0.1$ cm^{-1}) is observed between transitions in the $^{24}Mg^+$ and $^{26}Mg^+$ ions. However, the resolution of the present experiment is not high enough to determine accurate values of the isotopic shifts. The spectra of individual isotopes are recorded by monitoring the ion signal in the appropriate range of flight times as a function of the tripled wavenumber of laser 3.

When detecting electrons in the PFI-ZEKE experiments, the various pulsed electric potentials used to field ionize the Rydberg ions and extract the PFI-ZEKE electrons are generated by an arbitrary waveform generator directly connected to the electrode stack. PFI-ZEKE photoelectron spectra are recorded by monitoring the field-ionization signal induced by specifically designed sequences of electric field pulses as a function of the tripled wavenumber of laser 3. The pulse sequences used for the different measurements presented in this article are described in Sec. 3. The potential differences across the stack typically range from +2 V to −10 V. A small background electron signal, located at the same time of flight as that of the ZEKE electrons but independent of the laser beams, is strongly reduced by applying a +10 V pulse prior to the pulsed excitation.

Assessment of the densities of neutral, singly- and doubly-charged species is of importance to characterize the experimental conditions. The number of Mg^+ and Mg^{2+} ions in the interaction volume is estimated by comparing the signal they generate on the MCP detector to that generated by a single ion. On average, about 600 Mg^+ ions are present in the cloud when the pulse energy of laser 1 is set to $E_1 = 50$ μJ, yielding a Mg^+ number density of the order of 10^4 cm^{-3}. Much larger pulse energies E_1 can be easily reached and yield much larger photoelectron and photoion signals. However, the large density of ions in the interaction region, and thus the large ion-induced stray electric fields, strongly perturb the measurements. All spectra presented below were thus recorded with $E_1 = 50$ μJ or less. For the typical pulse energies $E_2 = 150$ μJ

and $E_3 = 80$ μJ of lasers 2 and 3, only about 10 doubly-charged ions are generated, on average, in the interaction region at each experimental cycle. The Mg^{2+} ion densities are thus as low as 5×10^2 cm^{-3}. The number of PFI-ZEKE electrons observed at each laser shot is lower, typically 1 to 10, because of the energy selection. To improve the signal-to-noise ratio of the spectra, the signal is averaged over up to 100 experimental cycles at each wavenumber. To estimate the density of magnesium atoms in the beam, we use the signal from the two-photon, non-resonant ionization of ground-state magnesium by laser 2 (35745.10 cm^{-1}), which has a known cross section [20]. With a pulse energy $E_2 = 265$ μJ, we obtain a signal of ~ 10 Mg^+ ions per shot, and deduce that the number density of neutral Mg atoms in the photoexcitation volume is in the range $10^7 - 10^8$ cm^{-3}. Careful optimization of the source conditions yielded densities up to 10^9 cm^{-3}, but the experiments presented below were carried out with Mg densities of the order of 10^7 cm^{-3} in an effort to limit the number of charged particles in the interaction region. The particle densities presented above are order-of-magnitude estimates only.

3. Results

3.1. Rydberg excitation spectrum of Mg^+

The Rydberg excitation spectrum of $^{24}Mg^+$ recorded following resonant (2+1′) three-photon excitation via the 3d $^2D_{5/2}$ intermediate state is shown in Fig 2. It represents the yield of $^{24}Mg^{2+}$ ions produced by PFI recorded as a function of the total excitation wavenumber, *i.e.*, $2\tilde{\nu}_2 + \tilde{\nu}_3$. The spectrum consists of a single Rydberg series converging to the Mg^{2+} $^1S_0$ ionization threshold with principal quantum number n ranging from 51 to $\simeq 120$, above which the signal-to-noise ratio becomes insufficient to observe individual lines. Below $n = 51$, the strength of the pulsed electric field (≈ 520 V/cm, see Section 2) is not sufficient to ionize the Rydberg states. The intensity of the successive lines in the spectrum decreases in average as $1/n^3$, as expected from Rydberg scaling laws [16], which indicates that the excitation from the intermediate state to the Rydberg states is not saturated.

In the (2+1′) resonant excitation scheme used in the experiment, both p and f Rydberg series can be reached by one-photon excitation from the intermediate 3d $^2D_{5/2}$ state. The spectrum, however, only shows one series. To understand why this is the case and to assign the series, we have calculated the one-electron wave functions of the $3d_{5/2}$ state and those of the np and nf Rydberg states of Mg^+ with n ranging from 51 to 90 using the model potential of the Mg^{2+} $^1S_0$ ion core reported by Aymar *et al.* (see Eq. (3.25) and Table I of Ref. [21]). The calculations were performed on a dense spatial grid of constant step size using the Numerov algorithm. Fine-structure effects in the Rydberg states were neglected because no corresponding splittings were observed experimentally. The radial integrals involved in the dipole matrix elements $\langle n\ell|\mu|3d\rangle$ were computed using Simpson's rule. In the range of principal quantum numbers spanned by the experiment, the squares of the dipole matrix elements connecting the 3d state

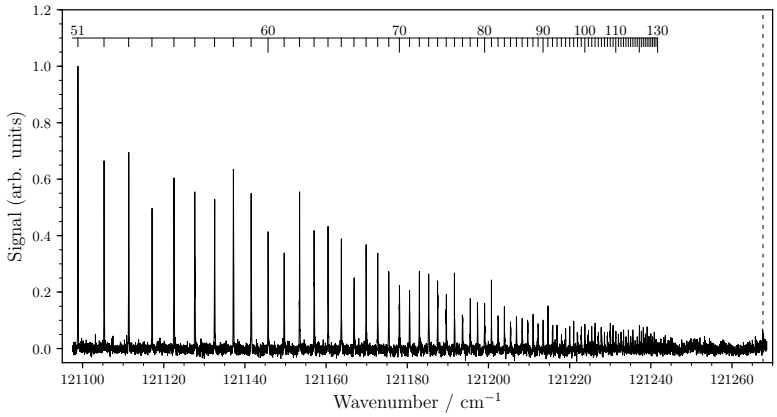

Figure 2: Spectrum of nf ^{2}F Rydberg series of $^{24}Mg^+$ recorded following (2+1′) three-photon excitation of ground state ions *via* the 3d $^2D_{5/2}$ intermediate state. The np ^{2}P series is not observable in the spectrum. The assignment bar at the top of the figure gives the principal quantum number of the nf series and the vertical dashed line indicates the position of the field-free ionization threshold of Mg^+ determined by Rydberg-series extrapolation (see text). The wavenumber scale is relative to the ground state of Mg^+.

to the np Rydberg states were found to be more than 40 times smaller than to the nf Rydberg states of the same n value. Because the angular parts of the dipole matrix elements are similar for both series, the large intensity difference between the two series is a consequence of the very different overlap between the initial and final radial wave functions. The calculations thus explain why the p Rydberg series is not detected experimentally and enable the unambiguous assignment of the observed series to the nf series.

The average full width at half maximum of the lines in the spectrum is 0.1 cm^{-1}, which we attribute to the bandwidth of the laser excitation. The contribution of Doppler and pressure broadening to the observed linewidth is negligible because the magnesium atoms are in a cold, collimated supersonic beam. Moreover, significant broadening by the Stark effect below $n = 120$ was avoided by the design of the excitation region [22] and by keeping the ion concentration in the photoexcitation volume as low as possible. The observed 0.1 cm^{-1} linewidth is compatible with the 0.05 cm^{-1} bandwidth of the fundamental beam of dye laser 3, which is frequency-tripled to access the Rydberg states of Mg^+. With the present bandwidth, Rydberg states with $n = 120$ could *not* be resolved in neutral Mg. In Mg^+, one benefits from the fact that the spacing between adjacent Rydberg states is proportional to Z_c^2/n^3, where $Z_c = 2$, instead of 1 for Mg.

The position of the field-free ionization threshold of $^{24}Mg^+$ was extracted from the spectrum presented in Fig. 2 by means of Rydberg-series extrapolation

using Rydberg's formula

$$\tilde{\nu}_{n\ell} = \frac{E_{\mathrm{I,\ Ryd}}}{hc} - \frac{4R_{^{24}\mathrm{Mg}}}{(n-\delta_\ell)^2}, \tag{4}$$

where $\tilde{\nu}_{n\ell}$ is the wavenumber associated with the energy difference between the Mg^+ Rydberg level with principal quantum number n and orbital angular momentum quantum number ℓ and the ground state of the ion. $R_{^{24}\mathrm{Mg}}$ is the mass-corrected Rydberg constant for ^{24}Mg and δ_ℓ is ℓ-dependent quantum defect. Eq. (4) accurately describes the Rydberg spectrum of Mg^+ below the Mg^{2+} $^1S_0$ ionization threshold because the excited electronic states of Mg^{2+} are energetically very distant and spectral perturbations caused by channel interactions are negligible [21]. The spectral position of each nf Rydberg state ($n = 51-120$) is determined by fitting the corresponding line profile in the measured spectrum with a Gaussian. These positions were then used to determine the field-free ionization threshold of Mg^+ ($E_{\mathrm{I,\ Ryd}}/hc = 121267.65\pm0.06$ cm^{-1}) and the quantum defect of the f-series ($\delta_\mathrm{f} = 0.0044(6)$) in a fit based on Eq. (4). The statistical uncertainty in the ionization threshold (0.003 cm^{-1}) is very small because the fit was performed using a large number of Rydberg-state positions. The major source of uncertainty is of systematic nature and is limited by the accuracy of 0.02 cm^{-1} of the wavemeter used to calibrate the fundamental wavenumber of laser 3. An overall uncertainty of 0.06 cm^{-1} results because the wavenumber of laser 3 is tripled to record the Rydberg spectrum. The value for the ionization threshold listed above agrees, within the error bars, with the value of 121267.64 ± 0.05 cm^{-1} determined by extrapolating the positions of low-lying ($n \leq 11$), high-ℓ ($\ell = 4-6$) levels [23]. The quantum defect of the f series is small, as expected for f states in an alkali-like system. For comparison, the quantum defect of the f Rydberg series in atomic sodium, which is isoelectronic to Mg^+, is 0.0016 [24]. We did not find other experimental or theoretical values for the quantum defect of high-lying nf states for comparison with our result. Using Ritz's expansion to extrapolate the quantum defects we extracted for low-lying f levels ($n = 4-10$) from term values reported in the NIST tables [19], we obtain a value of 0.0036 at $n = 51$, which is slightly smaller than our result.

3.2. PFI-ZEKE spectra

PFI-ZEKE-photoelectron spectra of Mg^+ recorded by (2+1′) three-photon excitation via the 3d $^2D_{5/2}$ intermediate state using a single field-ionization pulse of variable strength F applied ~ 4 μs after the laser pulses are displayed in Fig. 3(a). These spectra are ordered according to the amplitude of the pulsed field and are shifted along the vertical axis by an offset corresponding to the value of $\sqrt{F}$, given by the horizontal lines. The wavenumbers corresponding to the half-rise of the signal are marked by open circles. They were determined by fitting the low-wavenumber onset of the PFI-ZEKE signal with the logistic function

$$I(\tilde{\nu}) = \frac{I_{\max}}{1+\exp(-k(\tilde{\nu}-\tilde{\nu}_0))}, \tag{5}$$

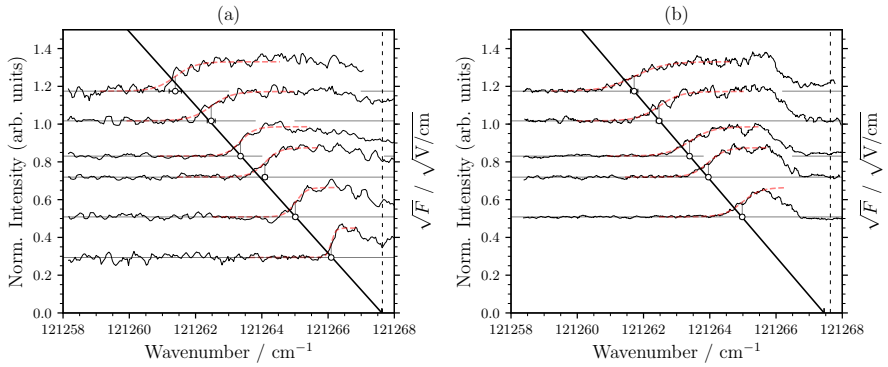

Figure 3: Dependence of the low-wavenumber onset of the PFI-ZEKE photoelectron signal at the Mg^{2+} $^1S_0$ threshold as a function of the amplitudes of the electric-field pulse. The spectra have been shifted along the vertical axis by an offset corresponding to $\sqrt{F}$ (see right axis labels). Panel (a): Experiments with a single pulse. Panel (b): Experiments with a discrimination pulse of 0.07 V/cm preceding the field ionization pulse (see text for details). The vertical dashed line indicates the position of the ionization threshold determined by Rydberg extrapolation (see Sec. 3.1).

where $\tilde{\nu}$ represents the wavenumber, $\tilde{\nu}_0$ denotes the half-rise position, $I_{\max}$ is the full signal strength and k determines the sharpness of the step. The fit results are depicted as dashed red lines and accurately describe the observed signal onsets. A linear regression of $\tilde{\nu}_0$ in dependence of $\sqrt{F}$ yields a coefficient $c = 5.07(7)$ in Eq. (1) and an extrapolated field-free ionization threshold of 121267.63(5) cm^{-1} (see diagonal line in Fig. 3(a) and Table 1). The numbers in parentheses represent one standard deviation of the fit results and also correspond to the standard deviation obtained by repeating the measurement several times. The estimated systematic uncertainties, coming mainly from stray electric fields in the excitation volume, are larger and amount to 0.3 for c and 0.3 cm^{-1} for the field-free ionization threshold.

The PFI signals in Fig. 3(a) do not sharply return to zero at the ionization threshold but extend into the ionization continuum. This behavior is attributed to the ions present in the excitation volume, which prevent the escape of slow electrons before the pulsed field is applied, and reduces the resolution of the photoelectron spectra. This artifact has been observed earlier in the PFI-ZEKE photoelectron spectra of *neutral* molecules and can be reduced by lowering the ion concentration in the probe volume [25]. In contrast to experiments with neutral species, there is an inherent positive ion concentration in PFI-ZEKE experiments on cations which cannot be eliminated without also eliminating the signal.

The trapping of slow electrons in the ion cloud can be avoided by using a discrimination pulse prior to the field-ionization pulse. However, the discrimination pulse also field-ionizes the highest Rydberg states according to Eq. (1). Fig. 3(b) presents PFI-ZEKE photoelectron spectra recorded with a discrimina-

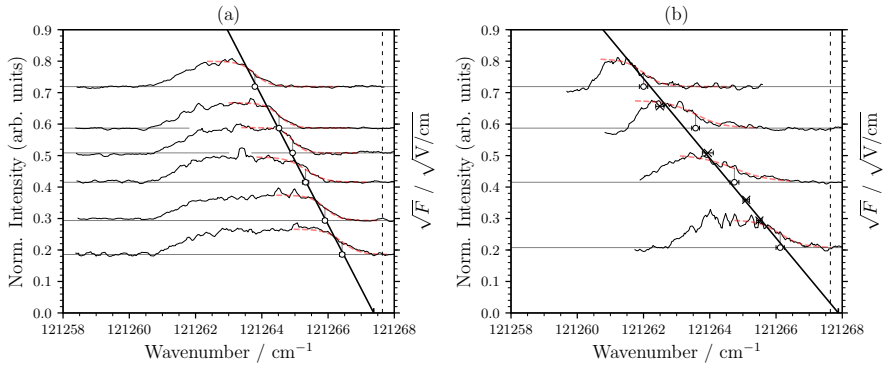

Figure 4: Dependence of the high-wavenumber edge of the PFI-ZEKE photoelectron signal at the Mg^{2+} $^1S_0$ threshold as a function of the strength of the discrimination electric field for (a) field-free laser excitation and (b) laser excitation overlapping with the discrimination field. The spectra are shifted vertically as explained in the caption of Fig. 3. Cross marks in panel (b) correspond to the positions of high-wavenumber edges determined at other field strengths from spectra that are not shown for the sake of clarity. The vertical dashed line denotes the ionization threshold obtained by Rydberg series extrapolation (see section 3.1).

tion pulse of 0.07 V/cm followed by field-ionization pulses of various strengths. These spectra are depicted as in Fig. 3(a) and exhibit the same field dependence of the low-frequency onset. A linear regression as described for Fig. 3(a) yields the results summarized in Table 1.

A two-pulse experiment also offers the possibility of examining the shift of the high-wavenumber edge of the PFI-ZEKE line as a function of the amplitude of the prepulse, as illustrated in Fig. 4(a). The PFI-ZEKE spectra shown in this figure were recorded with a field-ionization pulse of 1.7 V/cm. The spectra are presented as explained for Fig. 3 but the vertical shifts now correspond to the square root of the prepulse field strength. As expected, the slope (c in Eq. (1)) is the same as obtained for the spectra in Fig. 3 (see Table 1). The discrimination field can also be applied so that it overlaps with the laser excitation pulse. In this case we observe a different behavior, depicted in Fig. 4(b): The shift of the high-wavenumber edge is larger and can be described by a coefficient $c = 7.8 \pm 0.3$ in Eq. (1). A similar behavior is generally observed in PFI-ZEKE spectra of neutral molecules, however with c values of ~ 4 and ~ 6 for field-ionization following excitation under field-free conditions, and in the presence of a dc field, respectively [13, 26], as already mentioned in the introduction. The increased absolute value of the slopes observed in the PFI-ZEKE photoelectron spectra of Mg^+ compared to the field ionization of neutral Rydberg states is a consequence of the deeper Coulomb well of the doubly charged ion core. The simple classical field ionization model mentioned in the introduction would predict an increase of the value of c by a factor of $\sqrt{2}$. We observe a slightly smaller increase, by a factor of 1.25 instead of $\sqrt{2}$.

The best resolution achieved in the one- or two-pulse experiments described

Table 1: Wavenumber dependence of the low- and high-wavenumber edges of the PFI-ZEKE photoelectron signals and extrapolated field-free ionization thresholds.

	c in Eq. (1)	E_I/cm^{-1}
Rydberg-series extrapolation	—	121267.65 ± 0.06
Fig. 3(a)	5.1 ± 0.3	121267.6 ± 0.3
Fig. 3(b)	4.9 ± 0.3	121267.4 ± 0.3
Fig. 4(a)	5.0 ± 0.3	121267.5 ± 0.3
Fig. 4(b)	7.8 ± 0.3	121267.9 ± 0.3

above is 1.5 cm^{-1}, corresponding to the full width at half maximum of the line observed in the lowest trace of Fig. 3(b). A higher resolution can be reached by using multipulse field-ionization sequences of the type already used to record high-resolution PFI-ZEKE photoelectron spectra of neutral atoms and molecules [17]. The pulse sequence we used in this work is depicted in Fig. 5(a) and consists of a +0.4 V/cm discrimination pulse followed by a series of negative field steps going from −0.2 V/cm to −0.8 V/cm with a −50 mV/cm step size. The inversion of polarity after the discrimination pulse in this sequence converts the blue-shifted Rydberg-Stark states into red-shifted ones (and vice versa), a phenomenon referred to as Stark inversion below. Stark inversion is the key for achieving high resolution in PFI-ZEKE photoelectron spectroscopy, as explained in details in [17, 14].

Each of the field steps in the sequence releases electrons by field ionization, the strength of the corresponding electron signal being dependent on the laser excitation frequency. Indeed, the successive negative steps (with increasing field strength) ionize Rydberg states of decreasing principal quantum number. A typical example of an electron time-of-flight distribution obtained with this pulse sequence is displayed as the lower trace in Fig. 5(a). The different time intervals between the successive steps were chosen so as to be able to unambiguously correlate each electron signal with the field step that produced it.

Two sets of Mg^+ PFI-ZEKE photoelectron spectra recorded with this pulse sequence are shown in panels (b) and (c) of Fig. 5, the former recorded with a Mg^+ ion density ($\sim 3 \times 10^3$ cm^{-3}) roughly three times lower than the latter. The comparison of these two sets of measurements indicates that ions have a detrimental effect on the resolution. Whereas the narrowest lines in panel (b) have a full width at half maximum of about 0.3 cm^{-1}, those in panel (c) are at least twice as broad. The reason for the loss of resolution is that the field generated by the ions inhibits the Stark inversion, as was already demonstrated in earlier works [17]. This aspect represents a limitation of the application of PFI-ZEKE photoelectron spectroscopy to positively charged ions, because ions cannot be fully suppressed without also fully suppressing the photoelectron signal. The present results nevertheless demonstrate that an excellent resolution

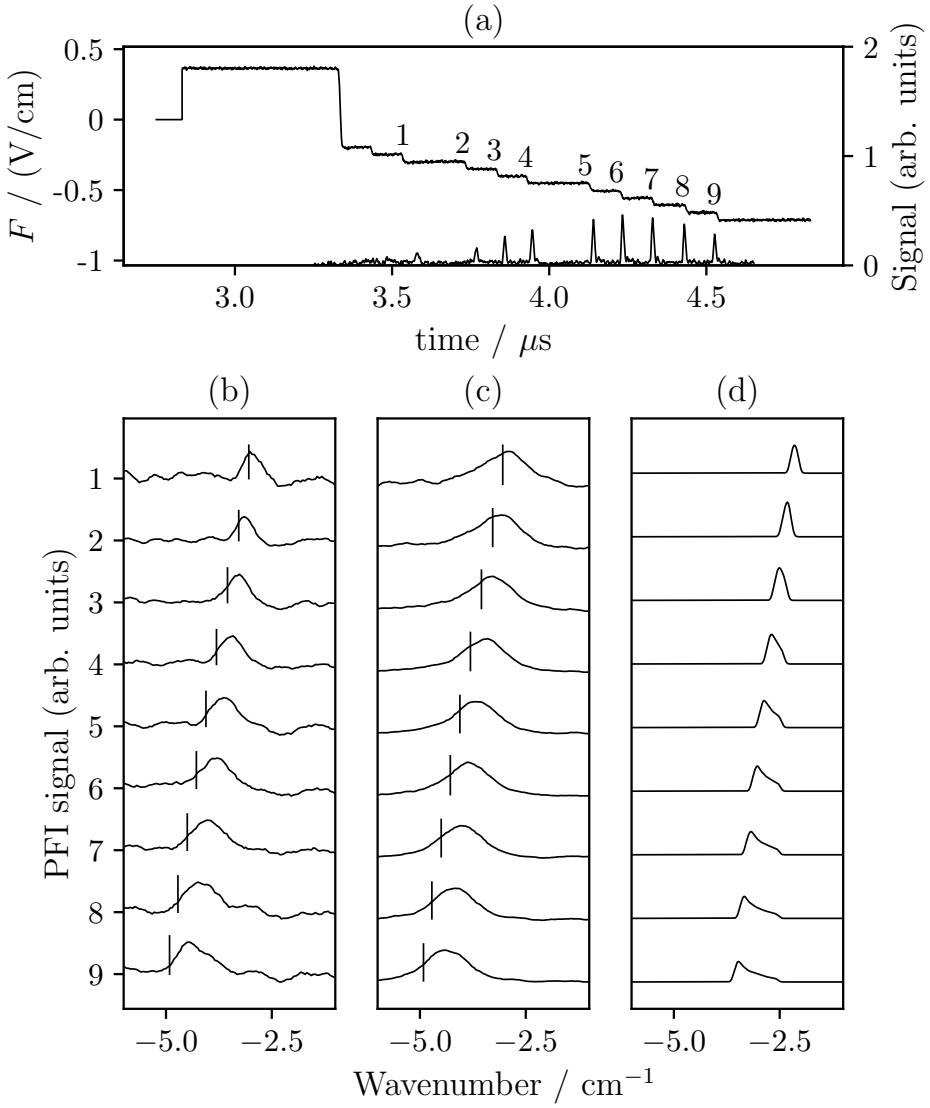

Figure 5: PFI-ZEKE photoelectron spectra of Mg^+ obtained with a multipulse field-ionization sequence with polarity inversion. (a) Field sequence (upper trace, left vertical axis) and electron time-of-flight distribution (lower trace, right vertical axis). (b) PFI-ZEKE photoelectron spectra recorded for a low Mg^+ ion concentration ($\sim 3\times10^3$ cm^{-3}). Labels on the left vertical axis indicate the corresponding field steps, as numbered in panel (a). The vertical bar in each spectrum shows the line position expected for a neutral species scaled by $\sqrt{2}$ (see text). (c) PFI-ZEKE photoelectron spectra recorded for a Mg^+ ion concentration of $\sim 9\times10^3$ cm^{-3}. (d) Theoretical PFI-ZEKE photoelectron spectra for a neutral atom/molecule, calculated using the field sequence shown in panel (a). In panels (b)-(d), the wavenumbers are given with respect to the field-free ionization threshold of Mg^+ at 121267.65 cm^{-1}.

(~ 0.3 cm^{-1}) can be achieved, several orders of magnitude better than the resolution obtained so far by double ionization of neutral molecules in combination with coincidence photoelectron spectroscopic methods (see Refs. [3, 4, 5, 6] and references therein). The only way to diminish the detrimental effect of ions on the resolution is to optimize the excitation efficiency to the high-Rydberg states detected by PFI. In the present case, we reach an excitation efficiency of about 1% by exploiting the nearly resonant nature of first excitation step in the two-photon excitation to the 3d ^{2}D$_{5/2}$ (see panel (b) in Fig. 1).

Panel (d) in Fig. 5 depicts PFI-ZEKE photoelectron spectra calculated for the different steps of the pulse sequence in the case of a neutral-atomic/molecular sample as described in Ref. [17]. The assumption that the shift of the PFI-ZEKE lines with respect to the field-free ionization threshold scales as $\sqrt{Z_c}$, as predicted by the simple, classical field-ionization model, would shift the maxima of the calculated spectra in panel (d) to the positions marked by the vertical bars in panels (b) and (c). These bars qualitatively describe the observed shifts although they tend to overestimate them, in particular for the last steps. This discrepancy and the discrepancies observed in the experiments employing one or two pulses (see discussion of Figs. 3 and 4 above) indicate a need for more detailed investigations of the field-ionization dynamics of ionic Rydberg states.

4. Conclusion

PFI-ZEKE photoelectron spectroscopy has been applied to a positively charged ion (Mg^+) generated by photoionization of a neutral precursor (Mg) in a supersonic beam. Experiments carried out at different densities of singly-charged ions and for a broad range of pulsed electric field ionization sequences have enabled us to characterize the main aspects of the field-ionization process and to identify the factors limiting the spectral resolution.

The application of PFI-ZEKE photoelectron spectroscopy to positively charged ions and to neutrals differ in several important respects: Firstly, the different charges of the ion cores alter the field-ionization properties. Compared to the situation encountered in the photoionization of neutrals, the shifts of the ionization thresholds of singly-charged ions induced by dc and pulsed electric fields of given strengths are larger. Simple classical considerations predict a uniform increase of the shifts by a factor of $\sqrt{2}$. Our results depart from this prediction, though only slightly. Further investigation, in particular on the theoretical side, may shed light on why this is the case. Secondly, the density of singly-charged ions in the photoexcitation volume, even when it is reduced to levels below 10^4/cm^{-3}, prevents the escape of slow electrons before the pulsed electric field is applied. Consequently, the lines in the photoelectron spectra extend into the ionization continuum when single electric field pulses are used. This undesirable effect can, however, be eliminated by applying a discrimination pulse prior to the field-ionization pulse. As is the case for neutral systems, choosing this discrimination pulse to be of opposite polarity to the field ionization pulse can be exploited to improve both the sensitivity and the resolution of the measurements

because of the inversion of Stark inversion [17]. However, thirdly, the inhomogeneous fields generated by the singly-charged ions in the photoexcitation volume can inhibit the Stark inversion and have a detrimental effect on the ultimate resolution that can be achieved by PFI-ZEKE photoelectron spectroscopy. To reach optimal conditions, it is thus necessary to carry out the experiment at the lowest possible ion densities and to achieve high photoexcitation efficiencies to the high Rydberg states. In the case of Mg^+, we have achieved photoexcitation efficiencies of about 1%, which enabled us to record PFI-ZEKE photoelectron spectra with a resolution (full width at half maximum) of 0.3 cm^{-1}.

The application of the method to molecules remains a challenge: the distribution of the ion population over several quantum states at a given (limited) total ion density will decrease the signal strength. The solution to this problem is known and consists in the preparation of state-selected ions by mass-analyzed threshold ionization [27, 28]. The photoexcitation efficiency of molecular ions to high Rydberg states may be reduced by unfavourable Franck-Condon factors and line broadening through predissociation, which will necessitate either powerful sources of short-wavelength radiation or optimized resonant multiphoton excitation sequences. The rapid progress of table-top VUV laser sources, synchrotrons and free-electron lasers makes us optimistic that PFI-ZEKE photoelectron spectra of molecular cations will be recorded soon.

Acknowledgments

It is a great pleasure to dedicate this article to Professor Helmut Schwarz on the occasion of his 75th birthday. We thank Dr. Urs Hollenstein for stimulating discussions and support, and Hansjürg Schmutz for technical assistance. This work was supported financially by the Swiss National Science Foundation (Project No. 200020-172620) and the European Research Council (ERC) under the European Union's Horizon 2020 research and innovation programme (Advanced Grant 743121).

References

[1] D. Schröder, H. Schwarz, Generation, stability, and reactivity of small, multiply charged ions in the gas phase, J. Phys. B: At. Mol. Phys. 27 (1994) 2191–2209.

[2] D. Mathur, Structure and dynamics of molecules in high charge states, Phys. Rep. 391 (2004) 1–118.

[3] H. Sabzyan, E. Keshavarz, Z. Noorisafa, Diatomic dications and dianions, J. Iran Chem. Soc. 11 (2014) 871–945.

[4] T. Arion, U. Herfgenhahn, Coincidence spectroscopy: Past, present and perspectives, J. Electron Spectrosc. Relat. Phenom. 200 (2015) 222–231.

[5] G. Dawber, A. G. McConkey, L. Avaldi, M. A. MacDonald, G. C. King, R. I. Hall, Threshold photoelectrons coincidence spectroscopy of doubly-charged ions of nitrogen, carbon monoxide, nitric oxide and oxygen, J. Phys. B: At. Mol. Phys. 27 (1994) 2191–2209.

[6] M. Hochlaf, R. I. Hall, F. Penent, H. Kjeldsen, P. Lablanquie, M. Lavollée, J. H. D. Eland, Threshold photoelectrons coincidence spectroscopy of N_2^{2+} and CO^{2+} ions, Chem. Phys. 207 (1996) 159–165.

[7] M. Lundqvist, D. Edvardsson, P. Baltzer, B. Wannberg, Doppler-free kinetic energy release spectrum of N_2^{2+} , J. Phys. B: At. Mol. Phys. 29 (1996) 1489–1499.

[8] A. S. Mullin, D. M. Szaflarski, K. Yokoyama, G. Gerber, Triplet state spectroscopy and photofragment dynamics of N_2^{2+}, J. Chem. Phys. 96 (1992) 3636–3648.

[9] S. G. Cox, A. D. J. Critchley, P. S. Kreynin, I. R. McNab, R. C. Shiell, F. E. Smith, High resolution spectroscopy and structure of molecular dications, Phys. Chem. Chem. Phys. 5 (2003) 663–676.

[10] M. L. Weichman, D. M. Neumark, Slow photoelectron velocity-map imaging of cryogenically cooled anions, Ann. Rev. Phys. Chem. 69 (2018) 101–124.

[11] G. Reiser, W. Habenicht, K. Müller-Dethlefs, E. W. Schlag, The ionization energy of nitric oxide, Chem. Phys. Lett. 152 (1988) 119–123.

[12] K. Müller-Dethlefs, E. W. Schlag, High-Resolution Zero Kinetic Energy (ZEKE) Photoelectron Spectroscopy of Molecular Systems, Ann. Rev. Phys. Chem. 42 (1991) 109–136.

[13] W. A. Chupka, Factors affecting lifetimes and resolution of Rydberg states observed in zero-electron-kinetic-energy spectroscopy, J. Chem. Phys. 98 (1993) 4520–4530.

[14] F. Merkt, S. Willitsch, U. Hollenstein, High-resolution photoelectron spectroscopy, in: M. Quack, F. Merkt (Eds.), Handbook of High-Resolution Spectroscopy, Vol. 3, John Wiley & Sons, Chichester, 2011, pp. 1617–1654. doi:10.1002/9780470749593.hrs071.

[15] R. F. Stebbings, F. B. Dunning (Eds.), Rydberg States of Atoms and Molecules, Cambridge University Press, Cambridge, 1983.

[16] T. F. Gallagher, Rydberg Atoms, Cambridge University Press, Cambridge, 1994.

[17] U. Hollenstein, R. Seiler, H. Schmutz, M. Andrist, F. Merkt, Selective field ionization of high Rydberg states: Application to zero-kinetic-energy photoelectron spectroscopy, J. Chem. Phys. 115 (2001) 5461–5469.

[18] D. E. Powers, S. G. Hansen, M. E. Geusic, A. C. Puiu, J. B. Hopkins, T. G. Dietz, M. A. Duncan, P. R. R. Langridge-Smith, R. E. Smalley, Supersonic metal cluster beams: laser photoionization studies of copper cluster (Cu2), J. Phys. Chem. 86 (1982) 2556–2560.

[19] A. Kramida, Y. Ralchenko, J. Reader, NIST ASD Team, NIST Atomic Spectra Database, http://www.nist.gov/pml/data/asd.cfm (2016). URL `http://physics.nist.gov/asd`

[20] R. Moccia, P. Spizzo, Atomic magnesium: III. Two-photon transition probabilities and ionisation cross sections: A valence-shell L 2 CI calculation, J. Phys. B At. Mol. Opt. Phys. 21 (1988) 1145–1154.

[21] M. Aymar, C. H. Greene, E. Luc-Koenig, Multichannel Rydberg spectroscopy of complex atoms, Rev. Mod. Phys. 68 (1996) 1015–1123.

[22] F. Merkt, A. Osterwalder, R. Seiler, R. Signorell, H. Palm, H. Schmutz, R. Gunzinger, High Rydberg states of argon: Stark effekt and field-ionization properties, J. Phys. B: At. Mol. Opt. Phys. 31 (1998) 1705–1724.

[23] V. Kaufman, W. C. Martin, Wavelengths and Energy Level Classifications of Magnesium Spectra for All Stages of Ionization (Mg I through Mg XII), J. Phys. Chem. Ref. Data 20 (1991) 83–152.

[24] S. Dyubko, V. Efremov, S. Podnos, X. Sun, K. B. MacAdam, Quantum defects of the sodium atom in f, g and h states, J. Phys. B: At. Mol. Opt. Phys. 30 (1997) 2345–2349.

[25] R. Signorell, F. Merkt, Artifacts in PFI-ZEKE Photoelectron Spectroscopy, in: C. Sándorfy (Ed.), The Role of Rydberg States in Spectroscopy and Photochemistry, Kluwer Academic Publishers, 1999, pp. 479–504. `doi:10.1007/0-306-46938-3\_17`.

[26] F. Merkt, Molecules in High Rydberg States, Ann. Rev. Phys. Chem. 48 (1997) 675–709.

[27] L. Zhu, P. Johnson, Mass analyzed threshold ionization spectroscopy, J. Chem. Phys. 94 (8) (1991) 5769–5771.

[28] F. Merkt, S. R. Mackenzie, T. P. Softley, Preparation of ions in selected rotational states by delayed pulsed field ionization, J. Chem. Phys. 99 (1993) 4213–4214.